



# OPEN A virus based vaccine combined with IL12 gene therapy eradicates aggressive melanoma

Nuša Brišar<sup>1,2</sup>, Katja Šuster<sup>1,3</sup>✉, Simona Kranjc Brezar<sup>4</sup> & Andrej Cör<sup>3,5</sup>

Our study introduces a novel bacteriophage-based vaccine strategy and evaluates its antitumor efficacy, both as a standalone therapy and in combination with gene electrotransfer (GET) of interleukin-12 (IL-12) plasmids. Using phage display technology, we produced engineered M13 bacteriophages expressing tumour peptides MAGE-A1, gp100, or MART-1/MELAN-A on the surface of the capsid. The therapeutic potential of bacteriophage vaccination alone or in combination with GET IL-12 was tested *in vivo* in a mouse malignant melanoma model. Response to treatment was further characterized by histological and immunohistochemical analyses of tumour tissue. No negative side effects were observed during treatment in mice. Engineered bacteriophage therapy significantly delayed tumour growth. GET IL-12 contributed to the therapeutic effect of engineered bacteriophages and increased tumour growth delay. Both therapies had a synergistic effect and led to complete responses in 30% of cases. Histological and immunohistochemical analyses have shown that both bacteriophage monotherapy and, especially in combination with GET IL-12, activate the immune system and increase the proportion of necrosis and the infiltration of macrophages, CD4+ and CD8+ T lymphocytes in tumours. For the first time, a cocktail of three engineered M13 bacteriophages displaying different melanoma-associated antigens with intratumoral IL-12 gene electrotransfer were applied, demonstrating a synergistic therapeutic effect in a highly aggressive melanoma model. Nanotechnological approaches, such as the use of genetically engineered bacteriophages, offer promising new avenues for the development of anti-tumour vaccines.

**Keywords** Immunotherapy, Bacteriophages, Bacteriophage display technology, Bacteriophage vaccine, Interleukin, Gene electrotransfer, Malignant melanoma

The incidence of melanoma is increasing worldwide, with more than 132,000 melanoma cases occurring globally each year<sup>1</sup>. For years, the cornerstones of melanoma treatment have been surgery, chemotherapy, and radiotherapy. The effectiveness of treatment is often limited by the aggressive nature of tumour growth and the development of resistance to therapy, and often falls short in the face of advanced-stage disease. In recent years, there has been rapid progress in understanding tumour biology, which has led to the development of more effective immunotherapeutic approaches, such as anti-tumour vaccines and gene therapy<sup>2,3</sup>.

Anti-tumour vaccines can activate the specific anti-tumour immune response and form a long-term memory effect to destroy tumour cells<sup>4</sup>. The advent of nanotechnology and nanoparticles, including prokaryotic viruses – bacteriophages with many intriguing characteristics for bioengineering – has opened up new avenues for the development of anti-tumour vaccines<sup>5</sup>. Bacteriophages are ubiquitous in nature and represent the most abundant organisms in various ecosystems, including the human body. Combining a relatively simple structure with the remarkable property of high intrinsic immunogenicity, bacteriophage research entered its second youth with the use of bacteriophages as targeted nanocarriers for antigen display in cancer therapy<sup>6–8</sup>.

With the advancement of phage display technology, synthetic biology, and nanotechnology, bacteriophages—particularly filamentous phages such as M13—have emerged as versatile nanocarriers for tumour antigen delivery and immunostimulation<sup>9</sup>. These engineered phages are capable of displaying multiple tumour-associated antigens, enhancing antigen-specific immune activation and promoting long-lasting immune memory<sup>10</sup>. Moreover, recent studies have highlighted the potential of phage-based vaccines to act as both delivery vehicles and immune adjuvants, due to their inherent immunogenicity<sup>11</sup>. When combined with other immunotherapeutic modalities

<sup>1</sup>Faculty of Health Sciences, University of Primorska, Koper, Slovenia. <sup>2</sup>Faculty of Medicine, University of Ljubljana, Ljubljana, Slovenia. <sup>3</sup>Scientific Research and Educational Department, Valdoltra Orthopaedic Hospital, Ankaran, Slovenia. <sup>4</sup>Department of Experimental Oncology, Institute of Oncology Ljubljana, Ljubljana, Slovenia. <sup>5</sup>Faculty of Education, University of Primorska, Koper, Slovenia. ✉email: katja.suster@ob-valdoltra.si

such as immune checkpoint inhibitors or cytokine gene therapy, bacteriophage vaccines can overcome tumour-induced immunosuppression and enhance therapeutic efficacy. These developments position bacteriophage-based immunotherapy at the forefront of next-generation cancer treatment strategies.

Bacteriophage vaccines can be combined with other immunotherapeutic treatment approaches, such as immunomodulators, including the cytokine interleukin 12 (IL-12)<sup>12,13</sup>. To overcome the limitations associated with the initial use of recombinant cytokine protein therapy, which resulted in unacceptable toxicity due to high cytokine doses, a gene therapy approach is being explored. In gene therapy, nucleic acids are introduced into the patient's cells to induce them to produce therapeutic proteins that trigger an immune response against tumours<sup>14,15</sup>. There are several methods for delivering nucleic acids, including electroporation, a physical method that has shown clinical applicability. When nucleic acids are delivered by this method, it is called gene electrotransfer (GET). Ongoing clinical trials are evaluating the safety and efficacy of IL-12 gene electrotransfer<sup>16,17</sup>.

This study aimed to prepare a bacteriophage vaccine with three tumour-associated antigens fused with pVIII and to evaluate its antitumour efficacy *in vivo* in a murine tumour model of malignant melanoma. In addition, the study aimed to assess the impact of combining the bacteriophage vaccine with adjuvant GET of plasmid encoding IL-12 on the therapeutic efficacy and to investigate the antitumour activity.

## Results

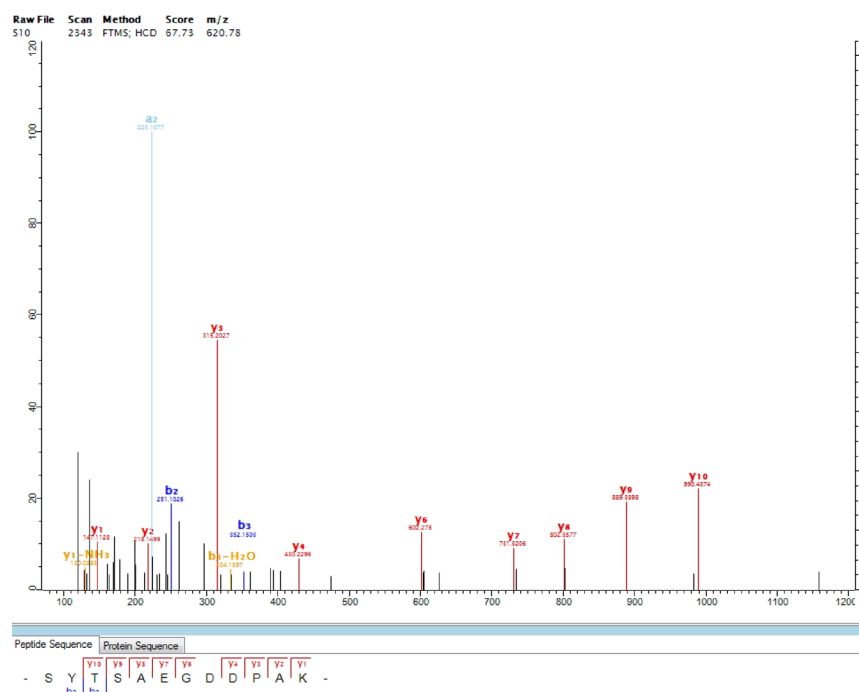
### Engineered M13 bacteriophage Preparation

During our previous study<sup>18</sup>, we described in detail the production of three different genetically engineered M13 bacteriophages displaying tumour peptides MAGE-A1, gp100, and MART-1 in fusion with pVIII. We verified that the tumour peptide transcript was present in the genome of the engineered bacteriophages, determined the titre of the bacteriophages, and checked the endotoxin levels. LC-MS/MS analysis was chosen to confirm recombinant fusion proteins due to their small size. We verified the coverage of the experimental fragmentation patterns with the theoretical spectra generated *in silico* from the UniProt proteomic database of bacteriophage M13 with recombinant proteins. Additionally, we examined the MS/MS spectra of the peptides identified within these recombinant proteins. A representative MS/MS spectrum of the SYTSAEGDDPAK peptide, identified in the recombinant fusion protein pVIII-MAGE-A1, is shown in Fig. 1. The well-annotated peaks and comprehensive coverage of b and y ions confirmed the peptide's identification.

### Therapeutic efficacy *in vivo*

During our *in vivo* experiments, we did not observe any changes in the behaviour of the mice after the treatment, and their body weight did not decrease during the time of the experiment. In the *in vivo* experiment, tumour growth was monitored to determine the anti-tumour efficacy of genetically engineered bacteriophage monotherapy or in combination with adjuvant IL-12.

Intraperitoneal administration of M13 bacteriophages has been shown to be an effective tumour growth inhibitor in early-stage disease. Tumours in the control group reached 10 mm<sup>3</sup> on average within 10 days,



while in the engineered bacteriophage-treated group, it took 21.3 days ( $p \leq 0.0001$ ). Bacteriophages presenting tumour peptides on their capsid were significantly more effective at inhibiting tumour growth than wild-type bacteriophages, where it took 14.3 days ( $p \leq 0.0001$ ) (Fig. 2).

The growth of the tumours was monitored until the volume reached 400 mm<sup>3</sup>, which was preset as the human endpoint of the experiment. In all groups where bacteriophage monotherapy was performed, a delay in tumour growth was observed compared to the control. In the control group, all tumours reached the humane endpoint within 16 to 20 days (median survival 17 days). In the wild-type bacteriophage group, all mice reached the endpoint within 26 days (median survival 24.5 days). In contrast, administration of genetically engineered bacteriophages prolonged mouse survival by 23.5 days, as mice reached the endpoint within 53 days (median survival 40.5 days). The prolonged survival was seen when combining bacteriophage therapy with GET of plasmid encoding IL-12 (pIL-12). Mice in the WT bacteriophages + GET pIL-12 group reached the experimental endpoint between 47 and 92 days (median survival 57 days), while in a group treated with engineered bacteriophages, the median survival increased from 40.5 days after the addition only of GET pIL-12 to 96.5 days and mice reached the experimental endpoint between 72 and 106 days. Moreover, combining genetically engineered bacteriophages and GET pIL-12 resulted in a 30% complete response rate (Fig. 3). In these mice, the appearance of vitiligo, hair, and skin depigmentation was observed in the area where the primary tumour was located (Fig. 4). No complete responses were observed in the bacteriophage monotherapy groups.

We demonstrated that engineered bacteriophage monotherapy statistically significantly ( $p \leq 0.0001$ ) prolonged the survival of mice compared to WT-bacteriophage monotherapy. Furthermore, adding adjuvant GET pIL-12 statistically significantly ( $p \leq 0.0001$ ) extended survival in mice treated with engineered bacteriophages compared to bacteriophage monotherapy alone. We have confirmed that combination therapy with engineered bacteriophages + GET pIL-12 had a synergistic effect. Combination therapy proved to be the most effective and resulted in longer survival than either monotherapy with engineered bacteriophages ( $p \leq 0.0001$ ) or monotherapy with GET pIL-12 ( $p \leq 0.01$ ) (Fig. 5).

### Tumour necrosis and immune infiltrate in tumours

On day 6 after the last bacteriophage treatment, tumours were harvested from three mice in each group, and the amount of necrosis in the tumours and the degree of immune cell infiltration were assessed in HE-stained slides. In the combination therapy group, tumours were very small at the time of sampling, having been replaced by a lymphocytic infiltrate. After bacteriophage monotherapy, areas of necrosis were seen throughout the tumours, and immune cell infiltration into the tumour tissue was also seen in viable parts of the tumours, although to a lesser extent compared to the combination therapy. In the control group, few immune cell infiltrations were observed, and parts of the tumours showed minimal necrosis, mostly in the central region, as a result of aggressive tumour growth (Fig. 6).

### Immunohistochemical evaluation of immune cell infiltration in tumour

The number of macrophages was significantly higher in the engineered bacteriophage monotherapy group or combined with GET pIL-12, compared to the control ( $p \leq 0.05$ ). The addition of adjuvant GET pIL-12 to engineered bacteriophage monotherapy resulted in a statistically significant increase in macrophage infiltration

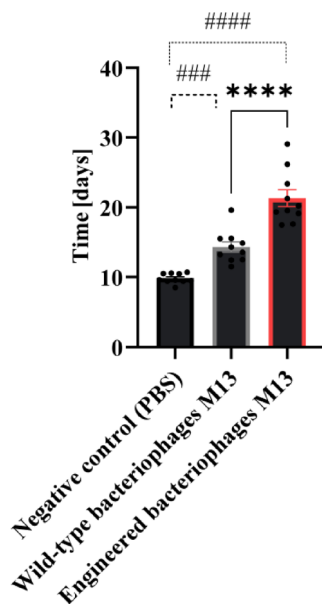


**Fig. 2.** Time of tumour outgrowth when tumour volume reached 10 mm<sup>3</sup>. Group differences were analysed with two-way analysis of variance (ANOVA), comparing groups to the negative control group (###,  $p \leq 0.001$ ; ####,  $p \leq 0.0001$ ) and comparing bacteriophage monotherapy groups (\*\*\*\*,  $p \leq 0.0001$ ), ( $n = 10$  mice in each group).

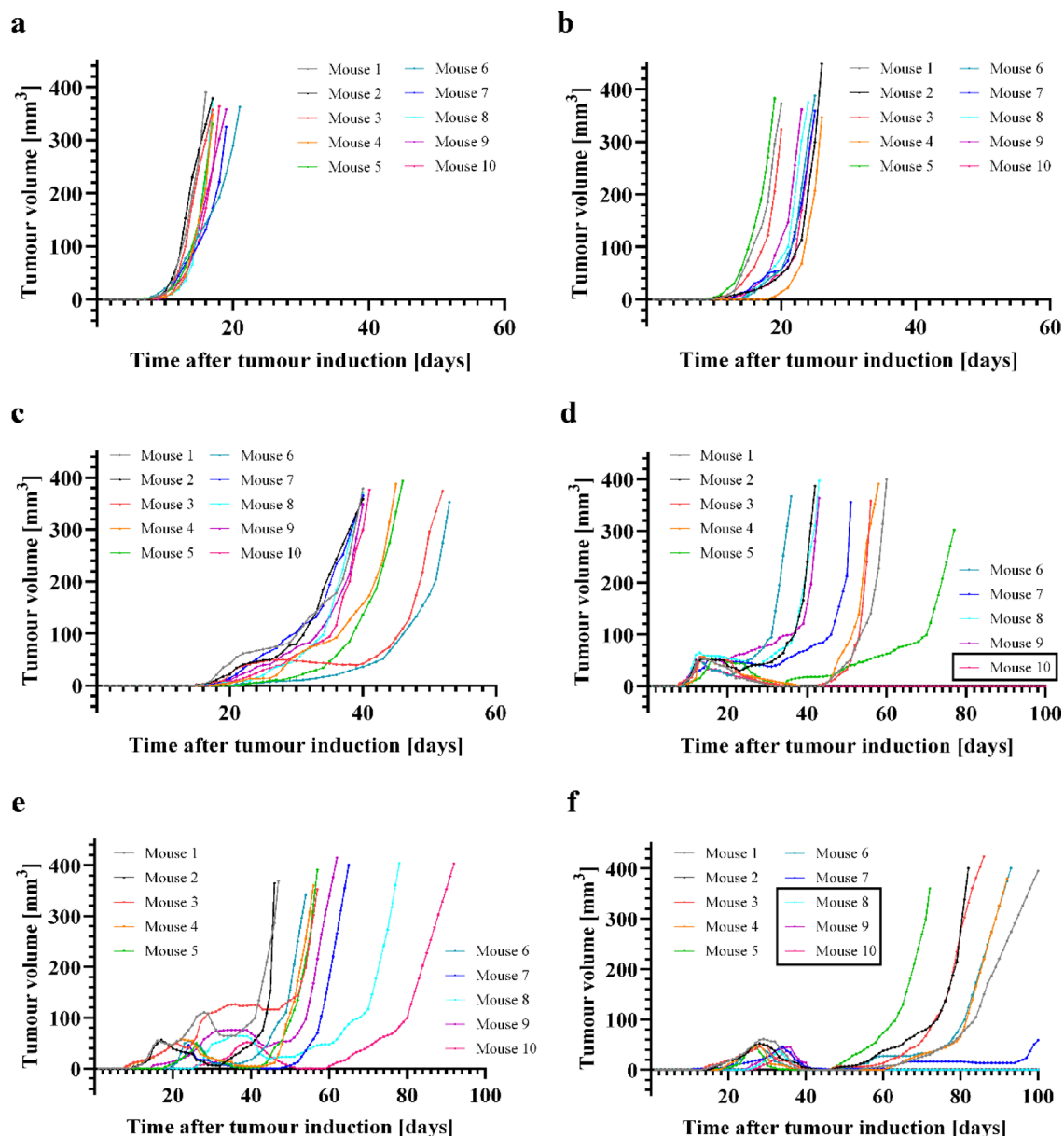


**Fig. 3.** Tumour growth curves of individual tumours ( $n = 10$  tumours) in (a) control group; (b) Wild-type bacteriophages group; (c) engineered bacteriophages group; (d) GET pIL-12 group; (e) WT bacteriophages + GET pIL-12 group; (f) engineered bacteriophages + GET pIL-12 group. Mice with complete responses are marked with a square.

( $p \leq 0.05$ ), with the highest levels seen in the combination therapy group ( $p \leq 0.05$ ). The number of CD8 + and CD4 + T lymphocyte cells was significantly higher in the genetically engineered bacteriophage monotherapy group or combined with GET pIL-12, compared to the control ( $p \leq 0.05$ ). GET pIL-12 increased T lymphocyte infiltration in the bacteriophage-treated groups, with the highest levels seen in the combination therapy group ( $p \leq 0.05$ ) (Fig. 7).

## Discussion

The present study describes the preparation of genetically engineered M13 filamentous bacteriophage virions expressing peptides derived from three different tumour-associated antigens. An in vivo experiment showed that a bacteriophage-based cancer vaccine is safe and generates an anti-tumour immune response capable of inhibiting tumour growth. Furthermore, combining engineered bacteriophages with gene electrotransfer of a plasmid encoding cytokine IL-12 was demonstrated to have a synergistic effect, resulting in enhanced immune cell infiltration into the tumour and contributing to the cure of malignant melanoma, however, without immune memory.



**Fig. 4.** Vitiligo observed in all cured mice in engineered bacteriophages + GET pIL-12 group.

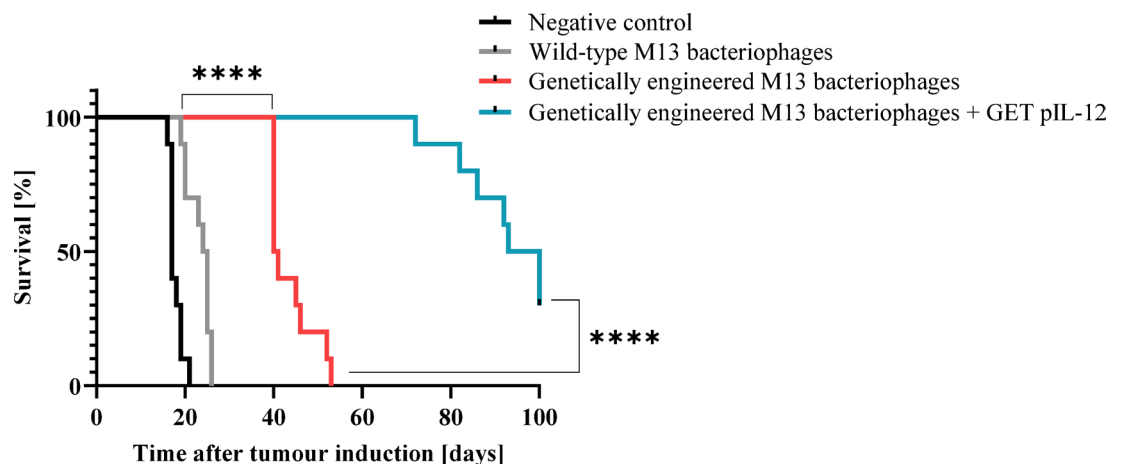


**Fig. 5.** Survival of mice with B16 F10 malignant melanoma treated with bacteriophage monotherapy or combined with adjuvant IL-12 gene electrotransfer. Data are presented using a Kaplan-Meier plot and were analysed with a Log-rank test. Statistically significant differences are indicated by asterisks (\*\*\*\*,  $p \leq 0.0001$ ;  $n = 10$  mice in each group).

The administration of a cocktail of engineered M13 bacteriophages expressing different tumour peptides on the bacteriophage capsid resulted in prolonged survival compared to a control group or a group receiving the wild-type bacteriophages. The selection of an appropriate antigen is crucial for the effectiveness of a cancer vaccine. In several studies, bacteriophage vaccines have been designed with bacteriophages displaying a single tumour antigen or its peptide<sup>19–21</sup>. Despite the promising therapeutic effects observed in this study, several resistance mechanisms inherent to immunotherapy could still pose challenges for durable tumour control. One common mechanism is the loss or downregulation of tumour-associated antigens, allowing tumour cells to evade immune detection. To mitigate this, our vaccine design incorporates three distinct melanoma-associated peptides (MAGE-A1, gp100, MART-1), aiming to broaden immune recognition and reduce the likelihood of immune escape. Another critical barrier is the immunosuppressive tumour microenvironment, which can impair T-cell function and lead to exhaustion. While the addition of IL-12 via gene electrotransfer enhances immune activation and tumour infiltration, it may not fully reverse the suppressive conditions within the tumour. Furthermore, the absence of long-term immune memory in our model suggests that booster strategies or combination with checkpoint inhibitors may be necessary to sustain antitumour immunity. Understanding and addressing these resistance mechanisms will be essential for the successful clinical translation of bacteriophage-based cancer immunotherapies.

Several lytic bacteriophages, including lambda<sup>22,23</sup>, T4<sup>21,24,25</sup>, and T7<sup>26,27</sup> have been proposed as delivery systems for proteins and peptides for cancer vaccines. However, we selected M13 filamentous bacteriophage over lytic counterparts due to its non-lytic nature, which allows easier production and purification<sup>28</sup>. Filamentous bacteriophages are recognized as inert antigen particles and naturally trigger an immunogenic response by activating both innate and adaptive immunity toward phage-displayed peptides. Their single-stranded DNA rich in CpG motifs can directly stimulate the toll-like receptor (TLR) innate immune pathway, leading to the



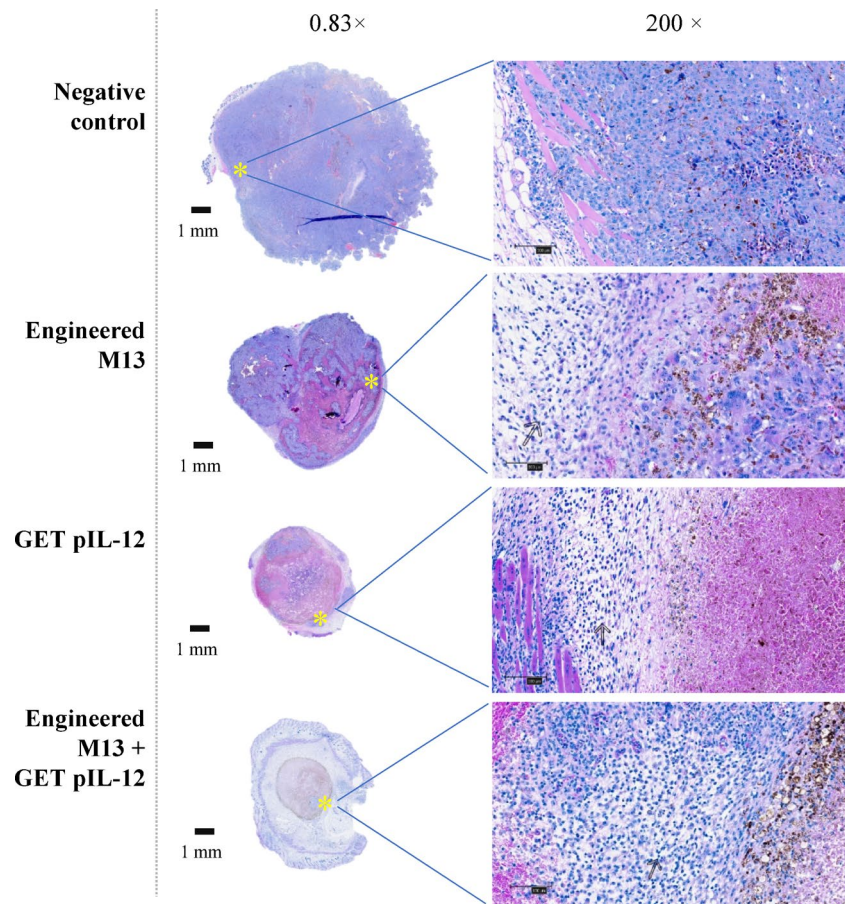


**Fig. 6.** Representative images of tumours stained with haematoxylin and eosin. Images were taken at 0.83× magnification (left). The scale bar represents 1 mm. Areas of immune cell infiltration are marked with yellow asterisks, and zoomed images of these infiltrations (right) were captured at 200× magnification ( $n = 3$  mice in each group).

induction of adaptive immune responses. M13 bacteriophages are taken up by antigen-presenting cells (APCs), promoting antigen release and cross-presentation, which subsequently activate CD4+ (MHCII) and CD8+ (MHCI) T-cell responses<sup>7</sup>.

In our study, we achieved complete responses using a combination of two immunotherapeutic approaches. Some other studies have reported complete responses also with engineered M13 bacteriophage monotherapy alone<sup>29</sup>. No complete responses after bacteriophage monotherapy in our study are likely due to the aggressive nature of malignant melanoma. For instance, in a study by Murgas et al.<sup>29</sup>, untreated BALB/c mice injected with CT26-CEA colon tumour cells reached the humane endpoint at 27 days, whereas in our study, control C57BL/6 mice reached the humane endpoint at just 17 days after B16 F10 tumour cell injection. CT26 is considered an immunologically 'hot' tumour that is likely to trigger a strong immune response with a good response to immunotherapy, whereas B16 F10 is a 'cold' tumour. In a study by Murgas et al.<sup>29</sup>, a single-chain variable antibody fragment against CEA (a carcinoembryonic antigen expressed in colorectal cancer) was fused to pIII of M13 bacteriophage. The therapy achieved 60% complete responses with systemic administration and 75% with intratumoural administration of the engineered bacteriophages. Wang et al.<sup>30</sup> used a bacteriophage vaccine targeting HER-2 and successfully prevented breast cancer relapse.

Mechanisms responsible for antitumor response line with the antitumor response were evaluated immunohistologically. We observed that engineered bacteriophage treatment increased the proportion of necrosis and the infiltration of immune cells into viable parts of the tumour tissue compared to the control group. Consistent with the literature, this is associated with a greater release of tumour antigens and consequently easier antigen presentation<sup>31</sup>. Engineered bacteriophages play an important role in activating the immune system, including macrophages, cytotoxic T lymphocytes, and T helper cells, which was also observed in our study. These observations were consistent with a slowing of tumour growth, further confirming the therapeutic effects of engineered bacteriophage treatment. Similarly, treatment with M13 bacteriophages in a preclinical breast cancer model resulted in enhanced tumor necrosis and improved immune cell infiltration<sup>32</sup>. Additionally, in studies involving a melanoma tumor model, therapy with a hybrid bacteriophage-DNA vaccine based on bacteriophage T7 demonstrated significant therapeutic potential and led to increased infiltration of inflammatory immune cells into the tumour tissue<sup>27</sup>.

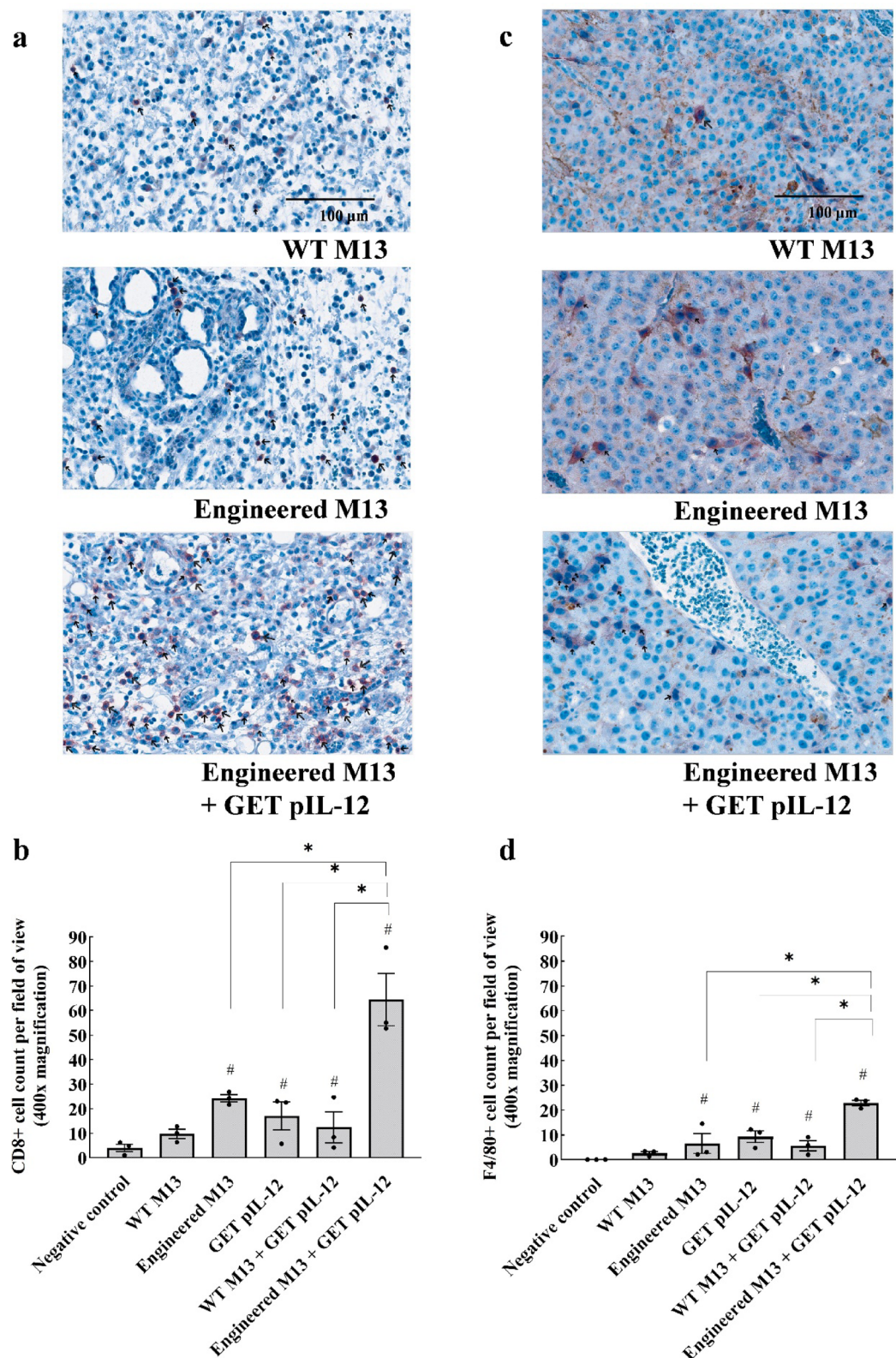


**Fig. 7.** (a) Representative images of malignant melanoma B16 F10 paraffin sections stained with anti-F4/80 monoclonal antibodies specific for macrophages. (b) Graph representing the number of macrophages in a field of view. (c) Representative images of malignant melanoma B16 F10 paraffin sections stained with anti-CD8 monoclonal antibodies specific for cytotoxic T lymphocytes. (d) Graph representing the number of CD8+ cells in a field of view. Immunopositive cells are stained red and marked with an arrow. The magnification on histological pictures (a and c) is 400x, and the scale bar is 100  $\mu$ m. Statistically significant differences were calculated using One-way ANOVA comparing therapeutic groups (\*,  $p \leq 0.05$ ) and comparing therapeutic groups to the negative control group (#,  $p \leq 0.05$ ).



The therapeutic potential of bacteriophages lies in their structure. Their small size and ease of genetic modification make them some of the most capable nanoparticles for delivering tumour antigens and eliciting a specific anti-tumour response. Their negligible tropism for mammalian cells and inability to proliferate in mammalian cells make them safe for medical use<sup>33</sup>. In our study, we also found no toxic effect of bacteriophages on B16 F10 cells (unpublished data). Thus, the increased knowledge of bacteriophage vaccines provides an opportunity to make them a routine tool for cancer immunotherapy in the future<sup>34</sup>.

The advantage of bacteriophage therapy is that it can be used with other therapeutic approaches that may be beneficial to improve treatment outcomes. Huang et al.<sup>35</sup> combined a bacteriophage vaccine with anti-PD1 therapy, demonstrating the potential of a synergistic immunotherapeutic approach. Our study combined bacteriophage therapy with the adjuvant cytokine IL-12 to enhance the anti-tumour effect. To ensure the local and sustained release of IL-12 within the tumour microenvironment and to avoid potential systemic side effects, we employed the method of intratumoral gene electrotransfer of a plasmid encoding IL-12. Various studies have optimized gene delivery protocols using electrical pulses to minimize tissue damage and improve gene transfer efficiency<sup>36–38</sup>. Some variables, such as the type of plasmid DNA (pDNA), the electrodes used, the parameters of the electrical pulses, and the type of tumour and tumour microenvironment, also influence the regulation of transgene expression and tissue damage during electroporation. In our study, when the tumours reached 50 mm<sup>3</sup>, a plasmid dose of 0.5 mg/ml was injected, and the tumours were subjected to electroporation, for which flat electrodes were chosen because of their less invasive nature. It was postulated that engineered bacteriophages expressing tumour peptides would elicit a sufficient antitumor response; therefore, cytokine IL-12 was added as an adjuvant to further boost the immune system. For the transfer of a larger plasmid molecule encoding IL-12, the protocol 600 V/cm, 5 ms, 1 Hz was selected, as it is commonly used for the delivery of genetic material.

Both monotherapy with GET pIL-12 and its integration into combination therapeutic strategies have demonstrated efficacy across various histologically diverse tumours in preclinical and clinical studies<sup>39–43</sup>. To the best of our knowledge, our research introduces a novel strategy that combines engineered bacteriophage virions displaying tumour peptides with GET of pDNA encoding IL-12 into tumour cells. Both therapies have synergistic effects. The engineered bacteriophages were observed to successfully activate the immune response and inhibit tumour growth, thereby prolonging the survival of the mice until the requisite volume for performing GET was reached. The administration of intratumoural GET pIL-12 subsequently enhances the immune response and prolongs mouse survival, as evidenced by the achievement of complete responses with the combination therapy. The literature presents evidence supporting the immune-activating effects of IL-12, which include enhancing the cytotoxicity of CD8 + T lymphocytes, promoting the differentiation of CD4 + T lymphocytes into Th1 cells, and stimulating IFN $\gamma$  production<sup>44</sup>. These actions collectively contribute to the enhancement of the tumour-suppressive response to therapy at multiple levels. Nevertheless, the antitumour efficacy is not solely attributable to the expression of the therapeutic transgene, interleukin-12, but also to the activation of interferon-beta (IFN- $\beta$ ) and IL-1 $\beta$  due to the introduction of foreign pDNA and the activation of DNA sensors<sup>45,46</sup>.

The study demonstrated that the combination of engineered bacteriophage therapy with GET pIL-12 was more efficacious than either monotherapy alone, resulting in enhanced lymphocyte infiltration into tumours. This finding is consistent with other research indicating that infiltration of tumours by effector immune cells is a key predictor of successful anticancer therapies. Kamensek et al.<sup>47</sup> tested the therapeutic potential of combining plasmids encoding cytokines IL-12 and TNF- $\alpha$ , achieving 79% survival in treated animals with melanoma, compared to 28.6% with IL-12 alone. In our study, monotherapy with GET pIL-12 (0.5 mg/ml) resulted in a 10% survival rate. Kamensek et al.<sup>48</sup> used a higher dose of pIL-12 (2 mg/ml) with GET pIL-12 administered twice.

The results of the study by Komel et al.<sup>49</sup>, which used the same concentration of pIL-12 (0.5 mg/ml), indicated comparable tumour growth outcomes following GET pIL-12 monotherapy. We believe that the selection of therapeutic regimen and, in particular, the dose of pIL-12 exerts a significant influence on the anti-tumour efficacy. A low dose of pIL-12 (0.5 mg/ml) has been demonstrated to be effective in combination with therapies with engineered bacteriophages. The rationale for this decision assumed that the immune system had already been stimulated with engineered bacteriophages.

In addition, electrical pulses have the potential to facilitate the infiltration of immune cells into tumours. Lower voltage but longer duration pulses can also induce cell death, release tumour antigens, and create an inflammatory environment that attracts immune cells<sup>50</sup>. The combination of electrical pulses with the introduction of a pDNA encoding IL-12 has been observed to increase the density of immune cells<sup>51</sup>. Histological analysis showed macrophage, CD4+, and CD8 + T cell infiltration in the GET pIL-12 monotherapy group, with a significantly higher presence in the group treated with both engineered bacteriophages and GET pIL-12. This combination therapy (vaccination and adjuvant) activates anti-tumour macrophages, enhances T-cell activity, and slows tumour growth. In surviving mice, the therapy-induced vitiligo indicates that the immune system targets melanoma antigens in melanocytes presented by bacteriophages. This indicates successful recruitment of immune cells to the immunologically “cold” B16 F10 tumour. Vitiligo has also been observed in patients with metastatic melanoma who have responded well to immunotherapy<sup>52,53</sup>.

While bacteriophage-based vaccines hold significant promise for cancer immunotherapy, their clinical translation faces several challenges. Regulatory hurdles remain a key concern, as agencies like the FDA and EMA require extensive safety and efficacy data for biologics, and the complexity of phage biology necessitates stringent quality control for manufacturing and standardization. The use of genetically modified bacteriophages introduces additional regulatory complexities, as biosafety concerns and containment measures must be addressed to comply with existing frameworks governing genetic engineering. The limited number of clinical trials on phage-based cancer vaccines underscores the need for further research to establish their efficacy, optimal dosing strategies, and potential synergies with existing immunotherapies. To advance bacteriophage-based vaccines into routine clinical use, future research should focus on refining genetic modifications for



enhanced safety and efficacy, developing scalable and cost-effective production methods, and conducting large-scale clinical trials to validate their therapeutic potential.

## Conclusion

Our study demonstrated that engineered M13 bacteriophage monotherapy prolonged survival of treated animals and effects survival in combination with other therapies, highlighting their potential as effective therapeutics. With their unique structure and genetic modifiability, bacteriophages serve as excellent carriers for tumour antigens, facilitating targeted antitumor responses. Their natural adjuvant properties activate both innate and acquired immunity, while they are safe for medical use. Nonetheless, engineered bacteriophages can be combined with other immunotherapeutic approaches. Despite initial research of bacteriophage vaccines in oncology and a basic understanding of the interactions between bacteriophages and the human immune system, challenges remain in the use of bacteriophages to treat cancer. Further studies are necessary to confirm the safety and efficacy of bacteriophage therapy in cancer treatment.

## Materials and methods

### Production of genetically engineered M13 filamentous bacteriophages

We have developed a bacteriophage vaccine comprising a cocktail of three distinct engineered M13 bacteriophages. Each of these bacteriophages express the tumour peptides MAGE-A1 (first phage), gp100 (second phage), and MART-1/MELAN-A (third phage) in fusion with the pVIII coat proteins.

The design and production of genetically engineered M13 bacteriophages expressing specific tumour peptides using phage display technology was prepared as previously reported<sup>18</sup>. Briefly, we first prepared three different recombinant phagemid vectors pCom8 (Plasmid#63889, Addgene, Watertown, MA, USA) expressing MAGE-A1<sub>161–169</sub> (EADPTGHSY), gp100<sub>25–33</sub> (EGSRNQDWL), and MART-1/MELAN-A<sub>26–35</sub> (EAAGIGILTV) tumour peptides in fusion with the pVIII coat proteins. Recombinant phagemids were transformed into chemically competent *Escherichia coli* XL2-Blue cells (Agilent Technologies, Santa Clara, CA, USA), and the correct insertion of peptides was determined by Sanger sequencing (Eurofins Genomics, Germany). Bacterial transformant colonies containing each recombinant phagemid were then coinfecting with the VCSM13 helper bacteriophage (Agilent Technologies, Santa Clara, CA, USA) and after overnight incubation, the engineered bacteriophages were recovered by Peg (Merck, Darmstadt, Germany)/NaCl (Carlo Erba Reagents, Milano, Italy) precipitation and centrifugation. Recombinant fusion proteins were identified by nano LC-MS/MS analysis.

We have optimised the production process for the propagation of M13 bacteriophages in large quantities and their further purification for in vivo experiments. This involved the application of different purification methods, including tangential flow filtration and anion exchange chromatography. At each purification stage, the presence of a tumour peptide transcript in the genome of the engineered bacteriophages was verified, the titre of the bacteriophages was determined by the plaque assay, and the endotoxin level was quantified by the LAL chromogenic assay in accordance with the pharmacopoeia method USP <85>/Ph. The bacteriophages were prepared in phosphate-buffered saline (PBS) at a concentration of 137 mM NaCl, 8.1 mM Na<sub>2</sub>HPO<sub>4</sub>, 2.7 mM KCl, 1.5 mM KH<sub>2</sub>PO<sub>4</sub>, pH = 7.4, for vaccination of the animals.

### Cell line

The B16 F10 murine malignant melanoma cell line (American Type Culture Collection, Manassas, VA, USA) was cultured in Dulbecco's modified Eagle's medium (DMEM; Gibco, Thermo Fisher Scientific, Waltham, MA, USA) supplemented with 10 mL/L L-glutamine (GlutaMAX; Gibco), 5% (v/v) fetal bovine serum (FBS; Gibco) and 10 mL/L penicillin-streptomycin (stock solution, 10,000 U/mL, Gibco) at 37 °C, 5% CO<sub>2</sub> atmosphere and 95% relative humidity. Cells were screened periodically for mycoplasma-free status using the MycoAlert™ PLUS Mycoplasma Detection Kit (Lonza Group Ltd, Basel, Switzerland) for confirmation.

### Recombinant plasmid encoding cytokine IL-12

Plasmid pORFmIL-12 (p40::p35) coding for mouse IL-2 was used. The plasmids were amplified in competent *E. coli* and purified using Endo Free Plasmid Giga Kit (Qiagen, Hilden, Germany) according to the manufacturer's protocol and dissolved in endotoxin-free water at a concentration of 0.5 mg/mL. The concentration of plasmid was measured using Qubit 3.0 Fluorometer (Thermo Fisher Scientific, Waltham, MA, USA). The identity of the plasmid was confirmed by restriction analysis and subsequent agarose gel electrophoresis. The purity of isolated plasmids was assessed using a microplate reader (Cytation 1, BioTek Instruments, Winooski, VT, USA) measuring the 260/280 and 260/230 absorbance ratios.

### Animals and tumour induction

In the experiment, 6–8 week-old female C57BL/6 NCrI mice (Charles River, Lecco, Italy) syngeneic for the selected B16 F10 tumour model were used. The mice were housed in specific pathogen-free (SPF) conditions in a carousel mouse IVC rack system (Animal Care Systems Inc., Centennial, CO, USA) under standard conditions of 20–24 °C, 55 ± 10% humidity, and on a controlled day-night cycle (12/12 h). Water and food were available *ad libitum*. The B16 F10 cells, obtained from in vitro culture, were resuspended in saline solution at a concentration of 5 × 10<sup>4</sup> cells/mL, and 100 µL of cell suspension was injected subcutaneously into the shaved right flank of mice. The mice were checked every day to evaluate their overall well-being. The mice were observed for any changes in their facial expressions and any unusual behaviours. Furthermore, the body weight of the mice was recorded three times weekly. All experiments were performed in accordance with relevant guidelines and regulations. Animal studies were performed in accordance with EU Directive (2010/63/EU) and with the approval of

Therapeutic group	Therapeutic regime
Group 1	Control group (PBS)
Group 2	Wild-type bacteriophage M13
Group 3	A cocktail of genetically engineered M13 bacteriophages
Group 4	GET pIL-12
Group 5	Wild-type bacteriophage M13 and GET pIL-12
Group 6	Cocktail of genetically engineered bacteriophages M13 and GET pIL-12

**Table 1.** Therapeutic groups.

the Veterinary Administration of the Ministry of Agriculture, Forestry and Food of the Republic of Slovenia (Approval No. U34401-3/2022/11). Tumour growth was recorded five days after the injection of tumour cells.

**In vivo experiments**

On day 5 after tumour induction, 96 mice were randomly assigned to six treatment groups (Table 1). Mice were administered a cocktail of three different genetically engineered bacteriophages via intraperitoneal injection ( $3 \times 10^{12}$  PFU/900 $\mu$ L PBS) three times at four-day intervals.

In the groups where the bacteriophage vaccine was combined with a GET of plasmids encoding the transgene IL-12, pIL-12 (0.5 mg/mL) was injected intratumorally at a tumour size of 50 mm<sup>3</sup>. Subsequently, two sets of four pulses were delivered to the tumour in perpendicular directions (600 V/cm, 5 ms, 1 Hz) using two parallel stainless-steel electrodes with a 6 mm gap between them via an electrical pulse generator (ELECTROcell B10 HVLV, Betatech, Saint-Orens-de-Gameville, France). During the procedure, animals were maintained under inhalation anaesthesia via inhalation with 1.5% isoflurane (Izofluran Torrex para 250 mL, Chiesi Slovenia) delivered via an oxygen concentrator (Supera Anesthesia Innovations, Estacada, OR, USA) at a flow rate of 1 L/min.

Twenty-four hours after the administration of pIL-12, the mice were injected with the fourth (final) dose of bacteriophage cocktail vaccine. The same time point was also employed for the groups of mice treated with bacteriophage monotherapy. At the end of the experiment, the mice were euthanized with cervical dislocation followed by exsanguination or CO<sub>2</sub> inhalation in a chamber.

**Tumour growth measurement**

After the therapy, tumour growth was monitored by measuring three orthogonal tumour diameters: the longest diameter (a), the diameter perpendicular to a (b), and the tumour thickness (c) three times a week using a Vernier calliper (model CD-15DAX, Mitutoyo, Japan). Tumor volume was calculated using the ellipsoid volume formula:  $(\pi \times abc)/6$ . The animals were euthanised when the tumour reached a predetermined humane endpoint, defined as a volume of 400 mm<sup>3</sup>. Mice that had a complete response (no palpable tumour 100 days after treatment) were considered cured (complete response).

**Histology and immunohistochemistry**

Tumour samples were harvested on day 6 after treatment, immersed overnight in 10% buffered formalin (BD Biosciences, San José, CA, USA), and then transferred to 70% ethanol (Sigma-Aldrich, St. Louis, MO, USA). Tumours were embedded in paraffin, and 4  $\mu$ m serial sections were prepared for histological and immunohistological staining. To assess the degree of necrosis and immune cell infiltration, tumour sections were stained with haematoxylin and eosin (HE). For IHC analysis, after deparaffinization, antigen retrieval was performed by incubation for 25 min in boiling sodium citrate buffer (10 mM sodium citrate, pH 6.0) supplemented with 0.5% Tween-20 detergent. Staining was continued with a commercially available rabbit-specific HRP-AEC IHC detection kit - micro-polymer (ab236468, Abcam, United Kingdom) according to the manufacturer's instructions. Sections were incubated with the primary antibodies in a humid chamber overnight at 4 °C, detecting the presence of macrophages (1:100 dilution, anti-F4/80 Ab, ab111101, Abcam), helper T lymphocytes (1:100 dilution, anti-CD4 + Ab, ab183685, Abcam), and cytotoxic T lymphocytes (1:200 dilution anti-CD8 Ab, ab209775, Abcam). Histological sections, unstained with the antibodies, were used as negative controls. Haematoxylin counterstaining was used for nuclear labelling.

The stained slides were examined under bright light using an Olympus BX-51 microscope (Olympus Corporation, Japan) connected to a DP72 CCD camera. To assess the proportion of necrosis, whole HE-stained tumours were imaged at 83 $\times$  magnification. To assess immune cell infiltration, tumours were imaged at 200 $\times$  magnification. To quantify the infiltration of macrophages, CD4 + and CD8 + T lymphocytes, three representative images of the viable part of the tumour tissue for each group were taken at 400 $\times$  magnification. Quantification of the positive signal was assessed in a blind fashion by 3 examiners using the freely available ImageJ image analysis software.

**Statistical analysis**

GraphPad Prism (GraphPad Software 10.1.2., Massachusetts, USA) was used for statistical data processing. All data were tested for normal distribution using the Shapiro-Wilk test. Differences between groups were determined by one-way or two-way analysis of variance (One/Two Way ANOVA). If the data were not normally distributed, differences between experimental groups were analysed using the non-parametric Kruskal-Wallis tests. When applicable, post hoc multiple comparisons were performed using Tukey's test (for ANOVA) or

Dunn's test (for non-parametric Kruskal–Wallis). The Kaplan–Meier survival curves were analysed using the log-rank test. Values of  $p \leq 0.05$  were considered statistically significant. The combination index (CI) was used to test the synergistic effect of two therapies, accounting for statistical variability in biological systems<sup>54</sup>.

## Data availability

The data analyzed during this study are presented and included in this article. Raw data are available from the author N.B., upon reasonable request.

Received: 7 February 2025; Accepted: 23 May 2025

Published online: 29 May 2025

## References

1. Radiation Ultraviolet (UV) radiation and skin cancer. (2024). [https://www.who.int/news-room/questions-and-answers/item/radiation-ultraviolet-\(uv\)-radiation-and-skin-cancer](https://www.who.int/news-room/questions-and-answers/item/radiation-ultraviolet-(uv)-radiation-and-skin-cancer)
2. Debela, D. T. et al. New approaches and procedures for cancer treatment: current perspectives. *SAGE Open. Med.* **9**, 20503121211034366 (2021).
3. Knight, A., Karapetyan, L. & Kirkwood, J. M. Immunotherapy in melanoma: recent advances and future directions. *Cancers (Basel)*. **15**, 1106 (2023).
4. Liu, J. et al. Cancer vaccines as promising immuno-therapeutics: platforms and current progress. *J. Hematol. Oncol.* **15**, 28 (2022).
5. Ragothaman, M. & Yoo, S. Y. Engineered Phage-Based Cancer vaccines: current advances and future directions. *Vaccines (Basel)*. **11**, 919 (2023).
6. Sartorius, R., D'Apice, L., Prisco, A. & De Berardinis, P. Arming Filamentous Bacteriophage, a Nature-Made Nanoparticle, for New Vaccine and Immunotherapeutic Strategies. *Pharmaceutics* **11**, (2019).
7. Goracci, M., Pignochino, Y. & Marchiò, S. Phage Display-Based nanotechnology applications in Cancer immunotherapy. *Molecules* **25**, 843 (2020).
8. González-Mora, A., Hernández-Pérez, J., Iqbal, H. M. N., Rito-Palomares, M. & Benavides, J. Bacteriophage-Based vaccines: A potent approach for antigen delivery. *Vaccines* **8**, 504 (2020).
9. Peltomaa, R., Benito-Peña, E., Barderas, R. & Moreno-Bondi, M. C. Phage display in the quest for new selective recognition elements for biosensors. *ACS Omega*. **4**, 11569–11580 (2019).
10. Hess, K. L. & Jewell, C. M. Phage display as a tool for vaccine and immunotherapy development. *Bioeng Transl Med* **5**, (2020).
11. Pizarro-Bauerle, J. & Ando, H. Engineered bacteriophages for practical applications. *Biol. Pharm. Bull.* **43**, 240–249 (2020).
12. Liu, C. et al. Cytokines: from clinical significance to quantification. *Adv. Sci.* **8**, 2004433 (2021).
13. Tripodi, L. et al. Systems Biology Approaches for the Improvement of Oncolytic Virus-Based Immunotherapies. *Cancers* **15**, (2023).
14. Berraondo, P. et al. Cytokines in clinical cancer immunotherapy. *Br. J. Cancer*. **120**, 6–15 (2019).
15. Lan, T., Chen, L. & Wei, X. Inflammatory cytokines in cancer: comprehensive Understanding and clinical progress in gene therapy. *Cells* **10**, 100 (2021).
16. Daud, A. I. et al. Phase I trial of Interleukin-12 plasmid electroporation in patients with metastatic melanoma. *JCO* **26**, 5896–5903 (2008).
17. Groselj, A. et al. Treatment of skin tumors with intratumoral Interleukin 12 gene electrotransfer in the head and neck region: a first-in-human clinical trial protocol. *Radiol. Oncol.* **56**, 398–408 (2022).
18. Brišar, N. et al. An engineered M13 filamentous nanoparticle as an antigen carrier for a malignant melanoma immunotherapeutic strategy. *Viruses* **16**, 232 (2024).
19. Fang, J. et al. The potential of phage display virions expressing malignant tumor specific antigen MAGE-A1 epitope in murine model. *Vaccine* **23**, 4860–4866 (2005).
20. Ren, S. et al. Antitumor activity of endogenous mFlt4 displayed on a T4 phage nanoparticle surface. *Acta Pharmacol. Sin.* **30**, 637–645 (2009).
21. Ren, S. et al. Inhibition of tumor angiogenesis in lung cancer by T4 phage surface displaying mVEGFR2 vaccine. *Vaccine* **29**, 5802–5811 (2011).
22. Pavoni, E., Vaccaro, P., D'Alessio, V., De Santis, R. & Minenkova, O. Simultaneous display of two large proteins on the head and tail of bacteriophage lambda. *BMC Biotechnol.* **13**, 79 (2013).
23. Razazan, A. et al. Lambda bacteriophage nanoparticles displaying GP2, a HER2/neu derived peptide, induce prophylactic and therapeutic activities against TUBO tumor model in mice. *Sci. Rep.* **9**, 2221 (2019).
24. Dabrowska, K. et al. Anticancer activity of bacteriophage T4 and its mutant HAP1 in mouse experimental tumour models. *Anticancer Res.* **24**, 3991–3995 (2004).
25. Sanmukh, S. G. et al. Bacteriophages M13 and T4 increase the expression of Anchorage-Dependent survival pathway genes and down regulate androgen receptor expression in LNCaP prostate cell line. *Viruses* **13**, 1754 (2021).
26. Shukla, G. S., Sun, Y. J., Pero, S. C., Sholler, G. S. & Krag, D. N. Immunization with tumor neoantigens displayed on T7 phage nanoparticles elicits plasma antibody and vaccine-draining lymph node B cell responses. *J. Immunol. Methods*. **460**, 51–62 (2018).
27. Hwang, Y. J. & Myung, H. Engineered bacteriophage T7 as a potent anticancer agent in vivo. *Front. Microbiol.* **11**, 491001 (2020).
28. Leili Aghebat-Maleki. Phage display as a promising approach for vaccine development. *Journal Biomedical Science* (2016).
29. Murgas, P. et al. A filamentous bacteriophage targeted to carcinoembryonic antigen induces tumor regression in mouse models of colorectal cancer. *Cancer Immunol. Immunother.* **67**, 183–193 (2018).
30. Wang, J. et al. HER2-Displaying M13 bacteriophages induce therapeutic immunity against breast Cancer. *Cancers* **14**, 4054 (2022).
31. Islam, M. S., Fan, J. & Pan, F. The power of phages: revolutionizing cancer treatment. *Front. Oncol.* **13**, 1290296 (2023).
32. Bartolacci, C. et al. Phage-Based Anti-HER2 vaccination can circumvent immune tolerance against breast cancer. *Cancer Immunol. Res.* **6**, 1486–1498 (2018).
33. Foglizzo, V. & Marchiò, S. Bacteriophages as therapeutic and diagnostic vehicles in Cancer. *Pharmaceutics (Basel)*. **14**, 161 (2021).
34. Palma, M. Aspects of Phage-Based vaccines for protein and epitope immunization. *Vaccines (Basel)*. **11**, 436 (2023).
35. Huang, S. et al. Reprogramming the genome of M13 bacteriophage for all-in-one personalized cancer vaccine. *Preprint At.* <https://doi.org/10.1101/2024.11.22.624916> (2024).
36. Tevz, G. et al. Controlled systemic release of interleukin-12 after gene electrotransfer to muscle for cancer gene therapy alone or in combination with ionizing radiation in murine sarcomas. *J. Gene Med.* **11**, 1125–1137 (2009).
37. Ursic, K., Kos, S., Kamensek, U., Cemazar, M. & Sersa, G. Peritumoral gene electrotransfer of interleukin-12 as an adjuvant immunotherapy to intratumoral electrochemotherapy for murine melanoma treatment. *Eur. J. Cancer*. **92**, S16–S17 (2018).
38. Tratar, L. Safety and efficacy of IL-12 plasmid DNA transfection into pig skin: supportive data for human clinical trials on gene therapy and vaccination. *IJMS* **25**, 3151 (2024).
39. Sedlar, A. et al. Radiosensitizing effect of intratumoral interleukin-12 gene electrotransfer in murine sarcoma. *BMC Cancer*. **13**, 38 (2013).

40. Tugues, S. et al. New insights into IL-12-mediated tumor suppression. *Cell. Death Differ.* **22**, 237–246 (2015).
41. Lamprecht Tratar, U. et al. Antitumor effect of antibiotic resistance gene-free plasmids encoding interleukin-12 in canine melanoma model. *Cancer Gene Ther.* **25**, 260–273 (2018).
42. Shi, G., Edelblute, C., Arpag, S., Lundberg, C. & Heller, R. IL-12 gene electrotransfer triggers a change in immune response within mouse tumors. *Cancers (Basel)*. **10**, 498 (2018).
43. Strojani, P. et al. Phase I trial of pIL12 plasmid intratumoral gene electrotransfer in patients with basal cell carcinoma in head and neck region. *Eur. J. Surg. Oncol.* **51**, 109574 (2025).
44. Lasek, W., Zagożdżon, R. & Jakobiński, M. Interleukin 12: still a promising candidate for tumor immunotherapy? *Cancer Immunol. Immunother.* **63**, 419–435 (2014).
45. Znidar, K., Bosnjak, M., Cemazar, M. & Heller, L. C. Cytosolic DNA sensor upregulation accompanies DNA electrotransfer in B16.F10 melanoma cells. *Mol. Ther. Nucleic Acids*. **5**, e322 (2016).
46. Znidar, K., Bosnjak, M., Jesenko, T., Heller, L. C. & Cemazar, M. Upregulation of DNA sensors in B16.F10 melanoma spheroid cells after electrotransfer of pDNA. *Technol. Cancer Res. Treat.* **17**, 1533033818780088 (2018).
47. Kamensek, U., Cemazar, M., Lamprecht Tratar, U., Ursic, K. & Sersa, G. Antitumor in situ vaccination effect of TNF $\alpha$  and IL-12 plasmid DNA electrotransfer in a murine melanoma model. *Cancer Immunol. Immunother.* **67**, 785–795 (2018).
48. Kamensek, U., Božič, T., Čemazar, M. & Švajger, U. Antitumor efficacy of Interleukin 12-Transfected mesenchymal stem cells in B16-F10 mouse melanoma tumor model. *Pharmaceutics* **17**, 278 (2025).
49. Komel, T. et al. Gene immunotherapy of Colon carcinoma with IL-2 and IL-12 using gene electrotransfer. *IJMS* **24**, 12900 (2023).
50. Chiarella, P., Fazio, V. M. & Signori, E. Electroporation in DNA vaccination protocols against cancer. *Curr. Drug Metab.* **14**, 291–299 (2013).
51. Lamprecht Tratar, U. et al. Gene electrotransfer of Plasmid-Encoding IL-12 recruits the M1 macrophages and Antigen-Presenting cells inducing the eradication of aggressive B16F10 murine melanoma. *Mediat. Inflamm.* **2017**, 1–11 (2017).
52. Teulings, H. E. et al. Vitiligo-Like depigmentation in patients with stage III-IV melanoma receiving immunotherapy and its association with survival: A systematic review and Meta-Analysis. *Journal Clin. Oncology: Official J. Am. Soc. Clin. Oncology* **33**, (2015).
53. Markelc, B. et al. Non-clinical evaluation of pmIL12 gene therapy for approval of the phase I clinical study. *Sci. Rep.* **14**, 22288 (2024).
54. Spector, S. A., Tyndall, M. & Kelley, E. Effects of acyclovir combined with other antiviral agents on human cytomegalovirus. *Am. J. Med.* **73**, 36–39 (1982).

## Author contributions

Conceptualization: N.B., K.Š., A.C. Investigation: N.B., S.K.B. Data Curation: N.B., S.K.B. Data Analysis and Visualization: N.B., K.Š., S.K.B., A.C. Methodology: N.B., K.Š., S.K.B., A.C. Supervision: A.C., K.Š. Original Draft Preparation: N.B. Writing – Review & Editing: K.Š., A.C., S.K.B., N.B. Funding acquisition: A.C. Resources: K.Š., A.C. All authors have read and agreed to the published version of the manuscript.

## Funding

This research was funded by the Slovenian Research and Innovation Agency (grant number P3-0003).

## Declarations

## Competing interests

The authors declare no competing interests.

## Ethics approval

The study was approved by the Veterinary Administration of the Ministry of Agriculture, Forestry and Food of the Republic of Slovenia (Approval No. U34401-3/2022/11). The study is reported in accordance with ARRIVE guidelines.

## Additional information

**Correspondence** and requests for materials should be addressed to K.Š.

**Reprints and permissions information** is available at [www.nature.com/reprints](http://www.nature.com/reprints).

**Correspondence to Katja Šuster.**

**Publisher's note** Springer Nature remains neutral with regard to jurisdictional claims in published maps and institutional affiliations.

**Open Access** This article is licensed under a Creative Commons Attribution-NonCommercial-NoDerivatives 4.0 International License, which permits any non-commercial use, sharing, distribution and reproduction in any medium or format, as long as you give appropriate credit to the original author(s) and the source, provide a link to the Creative Commons licence, and indicate if you modified the licensed material. You do not have permission under this licence to share adapted material derived from this article or parts of it. The images or other third party material in this article are included in the article's Creative Commons licence, unless indicated otherwise in a credit line to the material. If material is not included in the article's Creative Commons licence and your intended use is not permitted by statutory regulation or exceeds the permitted use, you will need to obtain permission directly from the copyright holder. To view a copy of this licence, visit <http://creativecommons.org/licenses/by-nc-nd/4.0/>.

© The Author(s) 2025